

# A Full Procedure to Model High Frequency Transformer Windings

R. Asensi, J.A. Cobos, O. García, R. Prieto and J. Uceda

Universidad Politécnica de Madrid  
División de Ingeniería Electrónica (DIE)  
C/ José Gutiérrez Abascal, 2 28006 Madrid SPAIN  
Tel.: 34-1-411 75 17 Fax: 34-1-564 59 66  
e-mail: cobos@upmdie.upm.es

**Abstract** - A full procedure to model high frequency magnetic components has been developed. A Finite Element Analysis (FEA) tool is used to compute the frequency behavior of the windings, taking into account geometry and frequency effects, like skin, proximity, interleaving, gap and end effects. The capacitive effects among the windings of the components are also taken into account. From these data, a model for the windings is developed by means of discrete components and differential equations that present the same frequency behavior as the actual component. Although the model has been developed for behavioral simulators, it can also be used in electrical simulators.

## INTRODUCTION

The switching frequency of the Switching Mode Power Supplies (SMPS) has increased in the last years in order to make smaller their magnetic components. The size of the magnetic components of the SMPS decreases as switching frequency increases (this size reduction has a limit determined by the thermal heating of the component). These higher working frequencies have generated a lot of research on the characterization and modeling of magnetic components. It is because the classic models do not take into account high frequency effects, both in the core and in the windings. A guide to several significant articles can be found in [1].

Furthermore, even for the simple models, the calculation of their parameters is only possible once the magnetic component has been built and tested. The user has not got a procedure to obtain, from the geometric description, an accurate model, frequency dependent, of the whole magnetic component. This would be very useful in order to simulate the whole SMPS before building it.

Recent papers propose models for the core, taking into account non-linearities and hysteresis effects - even considering minor loops - ([2-6]). Although eddy currents are not accurately modeled, it is possible to find commercial libraries with models for the core.

Regarding the windings, several papers have been published describing the high frequency effects that take place in them and proposing solutions for some of these problems.

However, the custom made nature of the windings and the difficulty to model all the effects for any electrical waveform have made winding modeling very inaccurate up to now. A scarcely studied topic is the capacitive effects that occur in the magnetic components. These effects are very important in high voltage converters, and in topologies that intend to integrate all the parasitic effects in the converter topology. There is not enough background work on this problem. (See [7]).

This work presents a procedure to calculate a model for a magnetic component from its geometric description. This model is made up of a set of differential equations and discrete components, capable of running in any behavioral simulator. It is also possible to represent the model as an electrical netlist, useful for electrical simulators. Since the frequency behavior is obtained by means of a FEA tool, skin, proximity, gap and end effects are taken into account for magnetic components with any number of windings and any winding strategy. Capacitive effects, both among the turns of a winding and between two windings are also taken into account by this model.

Better magnetic component models will help to have more accurate simulated electrical waveforms. The usefulness of the simulated electrical waveforms is very wide, from the design of the snubber of the power switch to the verification of the compliance of EMC standards.

## FLOWCHART OF THE MODEL GENERATION PROCEDURE

The key objective of this work is to develop models for the magnetic components. The models are generated directly from the geometric description of the magnetic component. This way, the time needed to redesign these components will be saved as it is not necessary to build them to get the model.

The modeling strategy proposed is represented in the flowchart of figure 1.

The first step is to produce a file that describes physically the magnetic component. The file is written in a format suitable for the FEA tool. The geometric information to build this file is extracted from a graphic module. In this graphic module, data

---

The present work was supported by the POWERCAD project (ESPRIT 6484) of the European Union.

0-7803-1859-5/94/\$4.00 © 1994 IEEE

about the magnetic component (number of layers, interconnections between the layers, kind of conductor, number

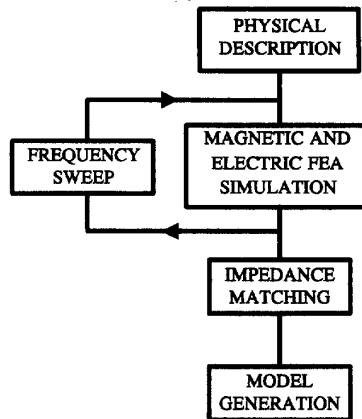


Fig. 1. Flowchart of the model generation procedure.

of turns, ...) is input. The module writes an ASCII file that contains the physical description of the component in a previously defined format and all the information necessary to produce the model (the parameters of the core model, the names of the terminals of the magnetic component, ...).

The second step is to perform an analysis with the FEA tool. In this step, two different analysis are performed. In the first one, a set of open circuit tests is simulated by means of the FEA tool. A current is introduced in a winding and the magnetic fields and current densities in the magnetic component are calculated in a frequency range. The lower frequency limit of the analysis is the working frequency of the component, and the upper frequency limit is several MHz, to take into account a high enough number of harmonic components of the electrical waveforms. These magnitudes are processed in order to get the frequency behavior of the component windings (losses and magnetic energy storage).

In order to model the energy storage because of the capacitive effects that take place in the magnetic component, an electrostatic analysis is also performed. This second analysis is performed in DC conditions. A voltage is imposed to the windings, and the electric fields in the magnetic component are calculated. The electric fields are processed in order to get the energy storage of the magnetic component as a function of the voltages imposed to its windings. The effect of the frequency on these capacitive effects will be studied in a future work, up to now constant capacitances have been employed.

The third step is the impedance matching. Given the losses and the magnetic energy storage data obtained in the AC analysis by means of the FEA tool, an impedance which frequency behavior is that of the AC data is calculated automatically.

The fourth step is the model generation. An ASCII file is written that is used by the behavioral simulator or electrical simulator.

As the model behavior changes with the frequency, this model is valid for non-sinusoidal high frequency waveforms. This file

is added to the netlist of the whole power converter in order to simulate the complete system.

## TWO WINDING MAGNETIC COMPONENT MODEL

The model that has been developed for this work consists of an ideal transformer (that accounts for the turns ratio of the component), a set of frequency dependent impedances (that account for the various effects of the frequency in the component), and a set of capacitors (in order to simulate the capacitive effects in the component). This model (for a two winding magnetic component) can be seen in figure 2.

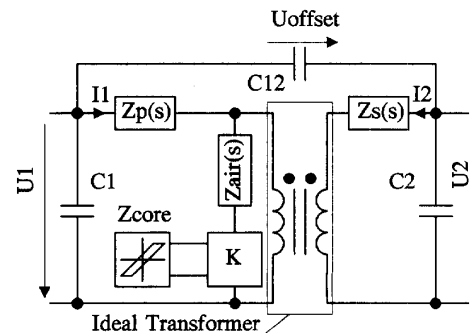


Fig. 2. Two winding magnetic component model.

There are two impedances,  $Z_{air}(s)$  and  $Z_{core}$ , instead of the magnetizing inductance of the core. The reason for this is the following: the flux that is common to both windings is composed of two parts. One of them circulates through the air common path and the other one through the core. The imaginary part of  $Z_{air}(s)$  represents the voltage produced by the flux that passes through the air (and the real part represents a fraction of the losses that appear in the windings as it is explained later on).  $Z_{core}$  represents the behavior of the core. All the odd effects that can appear in the gaps of the core are included in  $Z_{air}(s)$ , so, no restrictions about the flux behavior are made and all effects are taken into account. A commercial core model may be used once the flux that passes through it is determined.

If some circuit transformations are performed on the circuit of figure 2, the circuit of figure 3 is obtained.

The core model is connected to the circuit by means of a reluctances adaptor in order to get the proper value of the magnetizing inductance of the component. (The easiest case is that of the gapped inductors. The model would be composed of a series connection of an impedance that accounts for the air and an impedance that accounts for the core. The inductance is mainly determined by the gap, not by the core. In this case, the series core inductance is lower than the series air inductance).

The real parts of the impedances represent the losses in the windings. They are calculated by means of equation (1). (If  $I_1 = I_2 = I$ )

$$P = R_1 I^2 + R_2 I^2 + 2 R_{12} I^2 \quad (1)$$

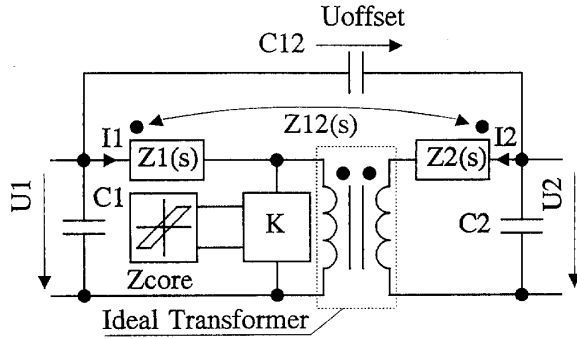


Fig. 3. Modified two winding magnetic component model.

- $R_1$  stands for the losses that appear in the primary winding when a current circulates through the primary winding plus the losses that are induced in the secondary winding. (There is not net current in the secondary winding).
- $R_2$  stands for the losses that appear in the secondary winding when a current circulates through the secondary winding plus the losses that are induced in the primary winding. (There is not net current in the primary winding).
- $R_{12}$  stands for the losses that appear in the primary winding when a current circulates through the secondary winding and there is current in the primary winding, and vice versa.

The magnetic energy storage in the component (except the core energy storage) is given by equation (2). (If  $I_1 = I_2 = I$ )

$$E = \frac{1}{2} L_1 I^2 + \frac{1}{2} L_2 I^2 + L_{12} I^2 \quad (2)$$

There is a similar explanation for equation (2), by using the imaginary part of the impedances of the model.

A similar analysis can be performed with the capacitive effects. In this case, a voltage drop between the primary and secondary terminals, and a voltage offset between the dotted terminals is taken into account. The capacitive energy storage in the magnetic component because of the capacitive effects is given by equation (3).

$$E = \frac{1}{2} C_1 U_1^2 + \frac{1}{2} C_2 U_2^2 + \frac{1}{2} C_{12} U_{offset}^2 \quad (3)$$

A method for extracting all the parameters of the model is presented in this paper. The main advantage of the model of figure 2 is that no assumption about the value of the magnetizing inductance is made (i.e. in order to group all the leakage energy storage in one term). This implies that the model is valid also for coupled inductors, where the effect of the magnetizing inductance cannot be neglected.

#### USING FEA TO MODEL THE MAGNETIC COMPONENT

Losses and energy storage in the magnetic component are calculated by means of a FEA tool. Superposition theorem is applied during the post-processing stage. The only part of the

magnetic component that is not linear is the magnetic core. If small magnetic flux densities are used, the magnetic component behavior is linear, so, superposition theorem can be applied. Linearity is considered for the post-processing of the electric fields because the permittivities of the materials of the magnetic component are assumed to be constant. They do not depend on the field intensity. The Maxwell equations are solved in the magnetic component by means of a FEA tool. Two different analysis are performed:

1. An AC analysis to calculate the magnetic fields. It is carried out in a specified frequency range. For a  $n$  winding component,  $n$  frequency sweeps are performed. In each of these analysis, a sinusoidal current (the same value,  $I$  amperes RMS, for all the windings) is introduced in each winding, one at a time. The superposition theorem says that the magnetic fields that appear in the component when certain currents are imposed to the windings are the sum of the fields that appear when only one of the windings is excited at a time.
2. A DC analysis to calculate the electric fields. For a  $n$  winding component,  $2n$  analysis are performed. In  $n$  of them, a voltage drop of  $U$  volts is imposed to a winding (one at a time) and  $0$  V to the other windings. These analysis are used to calculate the capacitance of a winding. In the other  $n$  analysis a constant voltage of  $U$  volts is imposed to a winding (one at a time) and  $0$  V to the other. Superposition theorem says that the electric fields that appear in the component when certain voltages are imposed to the windings are the sum of the fields that appear when only one of the windings is excited at a time.

Let us consider a  $n$  winding magnetic component. Some currents,  $I_i$ ,  $i = 1, 2, \dots, n$  enter winding  $i$ . The magnetic field,  $\vec{H}$ , that appears in the component is determined by the sum of some  $\vec{H}_i$  (the magnetic field that appears in the component when winding  $i$  is excited). Some current densities,  $\vec{J}_i$ , appear in winding  $i$  (it is composed of  $\vec{J}_{ii}$ , the current density that appears in winding  $i$  when winding  $i$  is excited and some  $\vec{J}_{ji}$ , the current density that appears in winding  $i$  when winding  $j$  is excited).

In a two winding magnetic component, equations (4-6) represent these magnitudes.

$$\vec{H} = \vec{H}_1 + \vec{H}_2 \quad (4)$$

$$\vec{J}_1 = \vec{J}_{11} + \vec{J}_{12} \quad (5)$$

$$\vec{J}_2 = \vec{J}_{22} + \vec{J}_{21} \quad (6)$$

The losses in the windings are given by equation (7). They are obtained by integrating the losses per unit of volume in all the conductors.

$$\begin{aligned}
P &= \iiint \frac{1}{\sigma} \vec{J} \cdot \vec{J}^* dv = \iiint \frac{1}{\sigma} [\vec{J}_1 \cdot \vec{J}_1^* + \vec{J}_2 \cdot \vec{J}_2^*] dv = \\
&= \iiint \frac{1}{\sigma} [\vec{J}_{11} \cdot \vec{J}_{11}^* + \vec{J}_{21} \cdot \vec{J}_{21}^*] dv + \\
&+ \iiint \frac{1}{\sigma} [\vec{J}_{12} \cdot \vec{J}_{12}^* + \vec{J}_{22} \cdot \vec{J}_{22}^*] dv + \\
&+ \iiint \frac{1}{\sigma} [\vec{J}_{11} \cdot \vec{J}_{12}^* + \vec{J}_{12} \cdot \vec{J}_{11}^* + \vec{J}_{21} \cdot \vec{J}_{22}^* + \vec{J}_{22} \cdot \vec{J}_{21}^*] dv
\end{aligned} \quad (7)$$

If the energy per unit of volume is integrated in all the component, the magnetic energy storage is obtained. This energy is given by equation (8).

$$\begin{aligned}
E &= \frac{1}{2} \iiint \mu \vec{H} \cdot \vec{H}^* dv = \\
&= \frac{1}{2} \iiint \mu \vec{H}_1 \cdot \vec{H}_1^* dv + \\
&+ \frac{1}{2} \iiint \mu \vec{H}_2 \cdot \vec{H}_2^* dv + \\
&+ \frac{1}{2} \iiint \mu [\vec{H}_1 \cdot \vec{H}_2^* + \vec{H}_2 \cdot \vec{H}_1^*] dv
\end{aligned} \quad (8)$$

It can be seen that some terms are null when one of the windings is not excited, and some terms appear independently of the current in the other winding.

If losses and magnetic energy are calculated in the circuit of figure 2, the winding losses and energy storage (excluding the core) are given in equations (1) and (2). Equations (9-14) are used to calculate the parameters of the model in a two winding magnetic component. They are obtained from equations (1), (2), (7) and (8).

$$R_1 = \frac{1}{I^2} \iiint \frac{1}{\sigma} [\vec{J}_{11} \cdot \vec{J}_{11}^* + \vec{J}_{21} \cdot \vec{J}_{21}^*] dv \quad (9)$$

$$R_2 = \frac{1}{I^2} \iiint \frac{1}{\sigma} [\vec{J}_{12} \cdot \vec{J}_{12}^* + \vec{J}_{22} \cdot \vec{J}_{22}^*] dv \quad (10)$$

$$R_{12} = \frac{1}{2I^2} \iiint \frac{1}{\sigma} [\vec{J}_{11} \cdot \vec{J}_{12}^* + \vec{J}_{12} \cdot \vec{J}_{11}^* + \vec{J}_{21} \cdot \vec{J}_{22}^* + \vec{J}_{22} \cdot \vec{J}_{21}^*] dv \quad (11)$$

$$L_1 = \frac{1}{I^2} \iiint \mu \vec{H}_1 \cdot \vec{H}_1^* dv \quad (12)$$

$$L_2 = \frac{1}{I^2} \iiint \mu \vec{H}_2 \cdot \vec{H}_2^* dv \quad (13)$$

$$L_{12} = \frac{1}{2I^2} \iiint \mu [\vec{H}_1 \cdot \vec{H}_2^* + \vec{H}_2 \cdot \vec{H}_1^*] dv \quad (14)$$

The energy equations do not consider the magnetic energy storage in the core (magnetic material). The available core model in the simulator is used to account for this energy as well

as for the losses. It is important to mention that during the FEA simulations, the core is assumed to be linear. So the non-linearities of the core are not taken into account during the windings model generation. However they are taken into account during the electrical simulation. As a matter of fact, core materials are not linear. This can produce errors in the simulations, but it is assumed that they are small if there is not saturation of the magnetic material (non-linear behavior). The effect of the non-linear behavior of the saturated core is assumed to be more important than the windings effect.

The energy storage in the gap and in the windings is included in the model in order to consider all the strain fluxes without any restriction.

If a U volts voltage drop is imposed to winding *i*, an electric field,  $\vec{E}_i$ , appears in the magnetic component. This electric field is used to calculate the capacitance associated to winding *i*. If a U volts offset voltage is applied to winding *i* and 0 volts to the other windings, some electric fields appear in the component,  $\vec{E}_{oi}$ . These fields are used to calculate the capacitance between two windings. It can be shown, as it was made in the study of the magnetic fields, that by applying superposition to the electric fields of the magnetic component, the capacitances of a two winding magnetic component are obtained by means of equations (15-17).

$$C_1 = \frac{1}{U^2} \iiint \epsilon \vec{E}_1 \cdot \vec{E}_1^* dv \quad (15)$$

$$C_2 = \frac{1}{U^2} \iiint \epsilon \vec{E}_2 \cdot \vec{E}_2^* dv \quad (16)$$

$$C_{12} = \frac{2}{U^2} \iiint \epsilon \vec{E}_{o1} \cdot \vec{E}_{o2}^* dv \quad (17)$$

#### THE EQUIVALENT IMPEDANCE

In order to obtain a stable behavior in the electrical simulation of the magnetic component, an impedance that verifies the properties of a real passive network is used. These properties can be found in network theory bibliography [8]. It is not necessary to determine the parameters of the electrical components of the impedance in order to simulate it, because the impedance equations can be introduced directly in the behavioral simulator. However, it can be done, in order to use the model in electrical simulators.

The generalized impedance that is used is given in equation (18), where NPF is the number of partial fractions that appear in the generalized impedance. This number determines the complexity of the network, and then the accuracy that can be obtained in the impedance matching step described in the last item.

This network is known as Foster's network, and its suitability for modeling the windings is shown below.

$$Z(s) = c_0 + c_1 s + \sum_{i=1}^{NPF} \frac{c_{2i} s}{s + c_{2i+1}} \quad (18)$$

After replacing the complex variable,  $s$ , with  $j\omega$ , the real and imaginary parts of the impedance are equations (19) and (20).

$$R(\omega) = c_0 + \sum_{i=1}^{NPF} \frac{c_{2i} \omega^2}{\omega^2 + c_{2i+1}^2} \quad (19)$$

$$X(\omega) = \omega L(\omega) = \omega \left[ c_1 + \sum_{i=1}^{NPF} \frac{c_{2i} c_{2i+1}}{\omega^2 + c_{2i+1}^2} \right] \quad (20)$$

If  $R(\omega)$  and  $L(\omega)$  are derived in  $\omega$ , equations (21) and (22) are obtained.

$$\frac{dR(\omega)}{d\omega} = \sum_{i=1}^{NPF} \frac{2c_{2i}c_{2i+1}\omega}{(\omega^2 + c_{2i+1}^2)^2} > 0 \quad (21)$$

$$\frac{dL(\omega)}{d\omega} = -\sum_{i=1}^{NPF} \frac{2c_{2i}c_{2i+1}\omega}{(\omega^2 + c_{2i+1}^2)^2} < 0 \quad (22)$$

(Being  $c_i > 0$  as it is explained later on).

In an actual winding, the windings losses increase with the frequency. In this impedance,  $R(\omega)$  presents the same behavior. In the same way, the energy storage in the magnetic field decreases with the frequency. In this impedance,  $L(\omega)$  presents the same behavior.

If all the  $c_i$  are not negative, all the conditions of an actual network are verified. If there are negative coefficients, it should be checked whether the stability conditions are verified. Only positive coefficients were considered in this work because the process is less time consuming and stability is assured.

#### IMPEDANCE MATCHING METHOD

To calculate the coefficients of the impedance given in equation (18), an estimation error given in equation (23) is minimized.

$$e = \sum_{i=1}^{ND} [(R_f(c_1, \dots, c_N, \omega_i) - R_d(\omega_i))^2 + (L_f(c_1, \dots, c_N, \omega_i) - L_d(\omega_i))^2] \quad (23)$$

In this equation:

- ND is the number of values to be approximated.
- $\omega_i$ ,  $R_d(\omega_i)$  and  $L_d(\omega_i)$  are the pulsating frequency, resistance and inductance of the data.
- $R_f(c_1, \dots, c_N, \omega)$ ,  $L_f(c_1, \dots, c_N, \omega)$  are equations (19) and (20).

To minimize the error function, the gradient method has been used. A C Language program has been written to implement this method. The program performs the impedance matching and the

model generation previously described. The approximation obtained in the calculation of the parameters of the impedance is shown in figures 4 and 5.

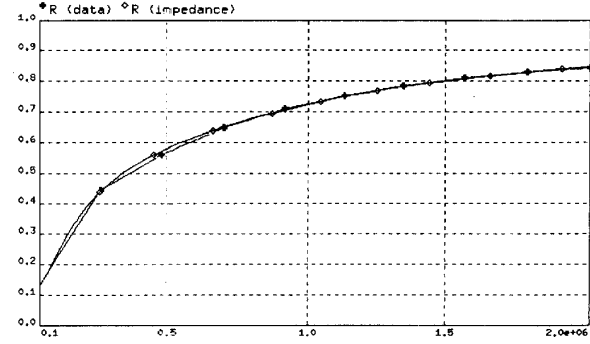


Fig. 4. Parameters calculation error. (Resistance).

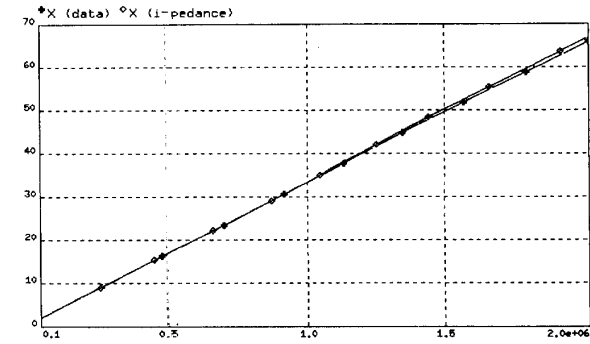


Fig. 5. Parameters calculation error. (Reactance).

#### MULTIWINDING MAGNETIC COMPONENTS

The technique used to model magnetic components with three or more windings consists on determining a set of coupled impedances and a set of capacitors.

The model of a three winding magnetic component can be seen in figure 6.

The parameters of the model can be obtained by applying superposition as it was made for the two winding magnetic components.

#### EXPERIMENTAL RESULTS

The above modeling procedure was tested by building some transformers and extracting their models. By means of an HP4195A impedance analyzer, the real and imaginary parts of the short circuit impedance of the transformers were measured. On the other hand, by means of a FEA tool and the program developed for this work, the models of the magnetic components were derived. Figures 7 and 8 show the approximation obtained by the calculated points (simulation in the behavioral simulator) to the actual points (obtained from the impedance analyzer) in

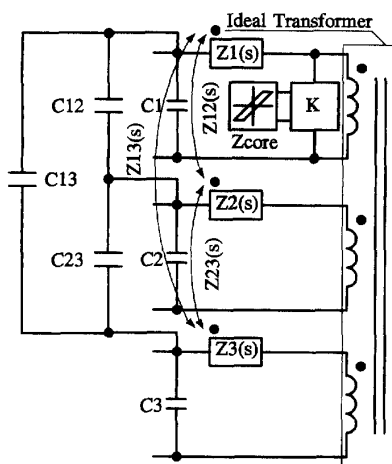


Fig. 6. Three winding magnetic component model.

the modeling of one of these transformers.

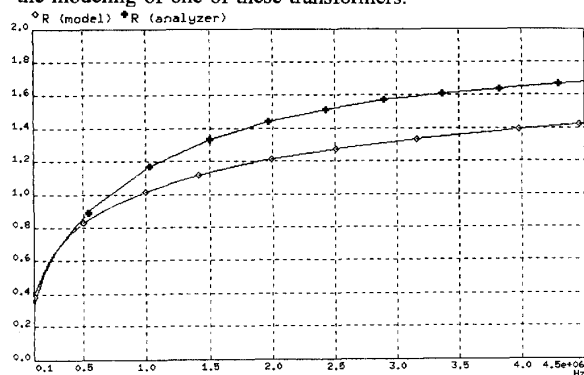


Fig. 7. Model and actual measurements. (Resistance).

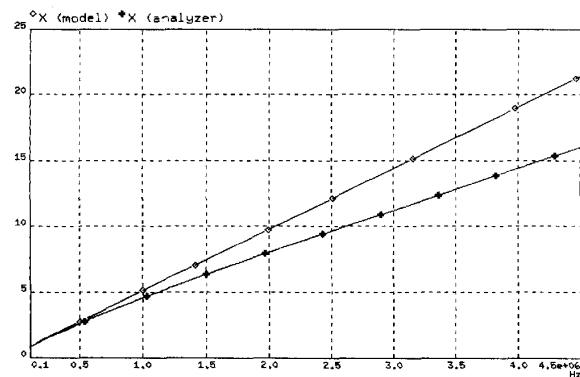


Fig. 8. Model and actual measurements. (Reactance).

The open circuit impedance of the same transformer was also obtained by means of the impedance analyzer and the behavioral simulator.

Figures 9 and 10 show the impedances obtained in these experiments.

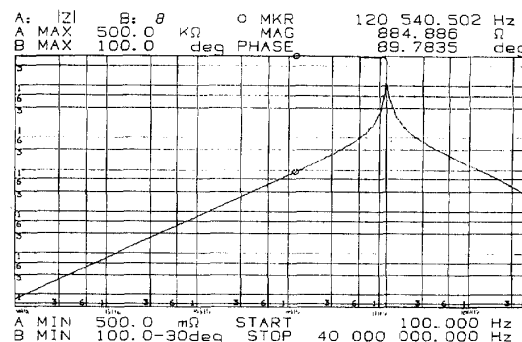


Fig. 9. Open circuit impedance of the real component.

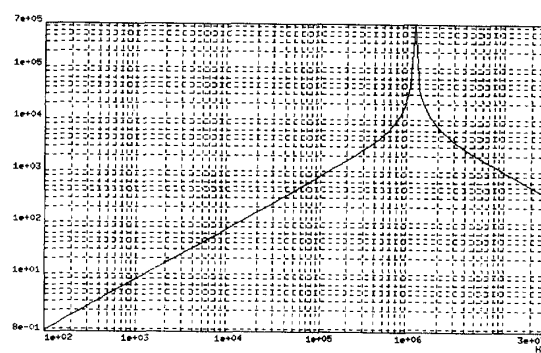


Fig. 10. Open circuit impedance of the model.

It can be seen the approximation obtained by the model at high frequencies. As the capacitances of the magnetic component are modeled, the resonance that takes place in the component between the magnetizing inductance and the capacitances of the windings can be detected by means of this model.

A SMPS was also built and tested. The topology is a forward converter.

The power transformer of the SMPS was modeled with a classic model (its parameters were obtained by means of the impedance analyzer), and the model developed for this work.

The whole SMPS, with both models, was simulated with a behavioral simulator. The actual waveforms of the SMPS were obtained in the laboratory by means of an oscilloscope.

Some electrical waveforms and experimental results are presented now. They were obtained from an oscilloscope in the laboratory, and from the electrical simulations in the workstation.

The electrical waveforms in the transistor are shown in figures 11, 12 and 13.

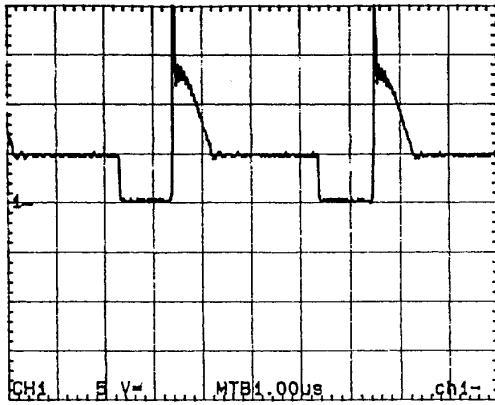


Fig. 11. Drain to source voltage (Oscilloscope).

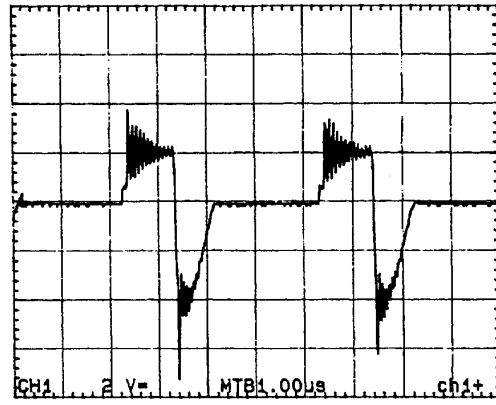


Fig. 14. Secondary voltage (Oscilloscope).

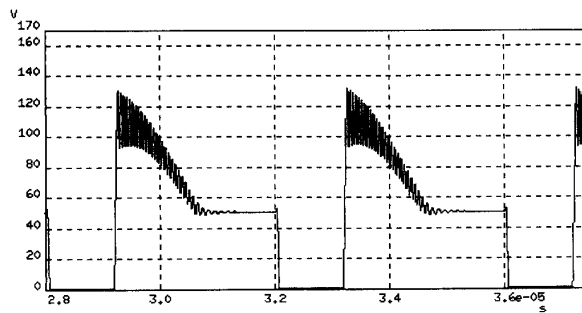


Fig. 12. Drain to source voltage. (Classic model).

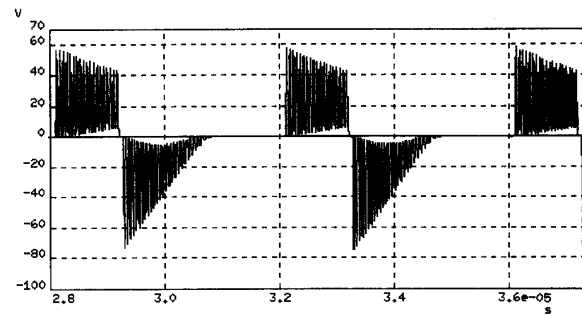


Fig. 15. Secondary voltage. (Classic model).

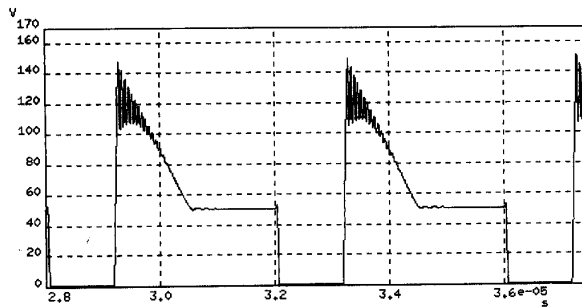


Fig. 13. Drain to source voltage. (Proposed model).

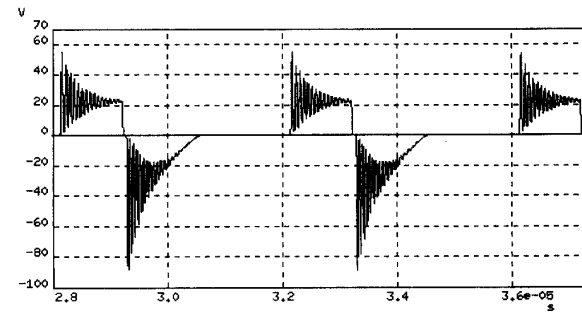


Fig. 16. Secondary voltage. (Proposed model).

And the voltage waveforms in the secondary of the transformer of the converter are shown in figures 14, 15 and 16.

It can be seen that the accuracy obtained by the proposed model is better than that of the classic model. The effect of the layout of the power converter board was simulated by means of some little inductances, the waveforms became more noisy.

In order to obtain good electrical simulations, it is necessary to develop models for the layout and the power semiconductors, as well as for the magnetic components.

## CONCLUSIONS

A full modeling technique for the windings of magnetic components has been derived. The model takes into account the frequency effects on the winding behavior. Thus, it is valid for non-sinusoidal electric waveforms. The capacitive effects are

also taken into account. Optimization techniques are used in order to determine the values of the parameters of the model. No user knowledge of the model generation process is necessary.

The whole model is obtained by means of the winding model developed plus a model for the effects that take place in the core.

# REFERENCES

- [1] A. M. Urling, V. A. Niemela, G. R. Skutt, T. G. Wilson. "Characterizing high frequency effects in transformers windings - A guide to several significant articles". IEEE APEC Record, 1989.
- [2] D.C. Jiles, D.L. Atherton. "Theory of ferromagnetic hysteresis". Journal of Magnetism and Magnetic Materials (1986).
- [3] K. H. Carpenter. "A differential equation approach to minor loops in the Jiles-Atherton hysteresis model". IEEE Transactions on Magnetics, Vol. 27, No. 6, November 1991.
- [4] K. H. Carpenter, S. Warren. "A wide bandwidth, dynamic hysteresis model for magnetization in soft ferrites". IEEE Transactions on Magnetics, Vol. 28, No. 5, September 1992.
- [5] J. H. Chan, A. Vladimirescu, Xiao-Chun Gao, P. Liebmman, J. Valainis. "Nonlinear transformer model for circuit simulation". IEEE Transactions on Computer-Aided Design, Vol. 10, No. 4, April, 1991.
- [6] I.D. Mayergoyz, G. Friedman. "Generalized Preisach model of hysteresis". IEEE Transactions on Magnetics, Vol. 24, No. 1, January 1988.
- [7] L. F. Casey, A. F. Goldberg, M. F. Schlecht. "Issues regarding the capacitance of 1-10 MHz transformers". IEEE APEC Record, February 1988.
- [8] W. Warzanskyj Poliscuk. *Métodos de Síntesis de Redes Lineales*. ETSI de Telecomunicaciones. Sección de Publicaciones.
- [9] A. F. Goldberg, J. G. Kassakian, M. F. Schlecht. "Issues related to 1-10 MHz transformer design". IEEE Transactions on Power Electronics. Vol 4, No. 2, April 1989.
- [10] B. Carsten. "High frequency conductor losses in switch mode magnetics". HFPC, May 1986 Proceedings.
- [11] A. F. Goldberg. "High field properties of Nickel-Zinc ferrites at 1-10 MHz". IEEE APEC Record, February 1988.
- [12] A. F. Goldberg, J. G. Kassakian, M. F. Schlecht. "Finite element analysis of copper loss in 1-10 MHz transformers". IEEE Transactions on Power Electronics. Vol. 4, No. 2, April 1989.
- [13] J. M. Lopera, A. M. Pernia, J. Díaz, J. M. Alonso, F. Nuño. "A complete transformer electric model, including frequency and geometry effects". IEEE PESC Record, 1992.
- [14] V. A. Niemela, G. R. Skutt, A. M. Urling, Yain-Nan Chang, T. G. Wilson, H. A. Owen, R. C. Wong. "Calculating the short-circuit impedances of a multiwinding transformer from its geometry". IEEE PESC Record, 1989.
- [15] V. A. Niemela, H. A. Owen, T. G. Wilson. "Cross-coupled-secondaries model for multiwinding transformers with parameters calculated from short-circuit impedances". IEEE PESC Record, 1990.
- [16] V. A. Niemela, H. A. Owen, Jr. and T. G. Wilson. "Frequency-independent-element cross-coupled-secondaries model for multiwinding transformers". IEEE PESC Record, 1992.